Predictive QE Models for PIC Codes

Using DFT, TMA, Delay Models, and Optical Models

K. L. Jensen[1], J. J. Petillo[2], D. Finkenstadt[3], N. A. Moody[4], A. Shabaev[1]

[1]Naval Research Laboratory, Washington DC
[2]Leidos Corp., Billerica, MA
[3]US Naval Academy. Annapolis MD
[4]Los Alamos National Laboratory. Los Alamos NM

Photocathode Physics for Photoinectors 2018: Theory Session
Oct 15-17, 2018 @ Time TBD, Los Alamos, NM
We thank Dr. O. Chubenko (GWU) for discussions and code development contributions

Sections Outline

General Thermal-Field-Photoemission Equation

RLD, FN, and FD are limits of GTFP:

$$J_{GTFP}(F,T) \equiv A_{RLD} T^2 N(n,s) \quad (1)$$

$$N(n,s) = n \int_{-\infty}^{\infty} \frac{\ln\left[1+e^{n(x-s)}\right]}{1+e^x} dx$$

$$\approx e^{-s} n^2 \Sigma\left(\frac{1}{n}\right) + e^{-ns}\Sigma(n) \quad (2)$$

$$N(n,-s) \approx \frac{1}{2}(ns)^2 + \zeta(2)\left(n^2+1\right) - N(n,s) \quad (3)$$

$$N(1,s) = (s+1)e^{-s} \quad (4)$$

$\beta_T = 1/k_B T$ and β_F are energy slope factors

$$n(F,T) \equiv \frac{\beta_T}{\beta_F}; \quad s(F,T) \equiv \beta_F(E_o - \mu) \quad (5)$$

$$\Sigma(x) \approx \frac{1+x^2}{1-x^2} + \left(\frac{\pi^2}{6} - 2\right)x^2 + \left(\frac{7\pi^4}{360} - 2\right)x^4 \quad (6)$$

$\Sigma(1) \to \infty$ so need $\Sigma(n)$ and $\Sigma(1/n)$ as $(n \to 1)$

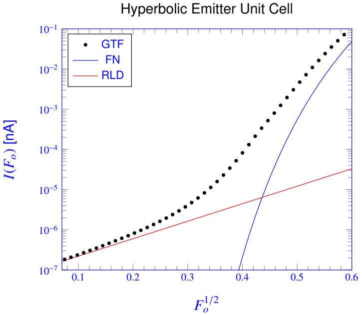

TF Current from hyperbolic emitter in triangular lattice (Slide 19) in RLD coordinates ($\ln(J)$ vs. $\sqrt{F}$). $\Phi = 2.3$ eV, $T = 1173$ K; field enhancement from Fig. 4.

Thermal (RLD), Field (FN), and Photoemission (FD) Regimes

RLD: $n \to 0$, $ns = \beta_T \phi$ FN: $n \to \infty$, $s = 4\sqrt{2m\Phi^3}\, v(y)/3\hbar F$ FD: $s \to -s$; $ns \to \beta_T(\hbar\omega - \phi)$

K.L. Jensen, *A Tutorial on Electron Sources*, IEEE Trans. Plas. Sci. **46(6)**, 1881 (2018).

Moments of a Distribution Function

Moments are integrals of k_j^n with a distribution:

$$QE = (1-R)\frac{M_1(k_z)}{2\,M_1\,(k)|_{D=1,\,f_\lambda=1}} \leftrightarrow M_n\left(\tilde{k}_j\right) = (2\pi)^{-3}\int d\vec{k}\left[\tilde{k}_j^n\right]\cdot[E]\cdot[T]\cdot[A]$$

The Parts

- Phase Space Element
- Momentum component
- Absorption (occupation)
- Transport (scattering factor)
- Emission (transmission prob)

$$d\vec{k} \rightarrow \left(\frac{2m}{\hbar^2}\right)^{3/2}\int_0^\infty E^{1/2}dE\int_0^{\pi/2}\sin\theta d\theta$$

$$[\tilde{k}_j^n] \rightarrow \left\{\frac{2m}{\hbar^2}\tilde{E}\cos^2\theta\right\}^{n/2}$$

$$[A] \rightarrow \left\{\begin{array}{c} f_{FD}(E)\,(1-f_{FD}(E+\hbar\omega)) \\ \Theta\left(\hbar\omega - E_g - E\right)\end{array}\right.$$

$$[T] \rightarrow f_\lambda(\cos\theta, p(E))$$

$$[E] \rightarrow D\left\{(E+\hbar\omega)\cos^2\theta\right\}$$

Relation to Dowell-Schmerge formula[a] for $\varepsilon_{n,rms}$

$$\varepsilon_{n,rms} = \frac{\hbar}{mc}\left(\frac{\rho_c}{2}\right)\sqrt{\frac{M_2\,(k_\perp)}{2M_0\,(k_\perp)}} \approx \frac{\rho_c}{2}\left[\frac{(\hbar\omega-\phi)}{3mc^2}\right]^{1/2}$$

[a] D.H. Dowell, J.F. Schmerge. "*QE and Thermal Emittance....*" Phys. Rev. ST Accel. Beams, **12(7)**, 074201, 2009.

Response Time and Scattering

Simplest Approximations: Only e^- to contribute to QE are

- unscattered = Fatal Approx
- Those for which $(E_x > V_o)$ = Fowler-DuBridge Approx
- Step function D(E) + simple δ, τ parameters

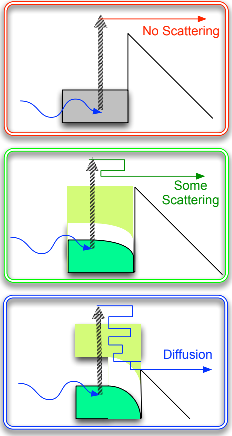

Fatal Approx Factor $(v_x = v\cos\theta)$

$$f_\lambda = \frac{\cos\theta}{\cos\theta + [\delta(\omega)/v(E)\tau(E)]} \tag{7}$$

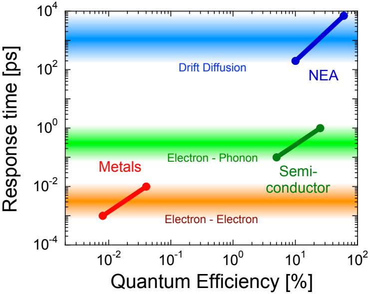

- Metals, $e-e$ scattering is fatal to emission (shares energy) so only unscattered electrons get to barrier
- Semiconductors, $e-p$ scattering changes E a small amount, so few scatterings do not impede emission
- Negative Electron Affinity: e^- thermalize to bottom of conduction band; can be emitted over an NEA surface

Sections Outline

"Conventional Wisdom" Surface Barrier

N.A. Moody, K.L. Jensen, A. Shabaev, S.G. Lambrakos, J. Smedley, D. Finkenstadt, I. Robel, J.M. Pietryga, Phys. Rev. Appl. (*accepted*) (2018).

$$QE = (1 - R(\omega)) \frac{\int_{E_a}^{\hbar\omega - E_g} EdE \int_{\sqrt{E_a/E}}^{1} xdx \, D_\Delta(Ex^2) \, f_\lambda(x, E)}{2 \int_0^{\hbar\omega - E_g} E \left[\int_0^1 dx \right] dE} \qquad (8)$$

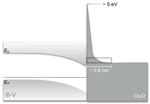

Barrier: high, thin triangle: let $s^2 \equiv (\hbar\omega - E_g - E_a)/E_a$ and $C \approx n(1 - R)/(1 + p)$ with $n = O(1)$

$$D_\triangle(E) \approx \frac{4[E(E - E_a)]^{1/2}}{(E^{1/2} + (E - E_a)^{1/2})^2} \rightarrow QE \approx \frac{2Cs^5}{(1 + s^2)(1 + \sqrt{1 + s^2})(s + \sqrt{1 + s^2})} \qquad (9)$$

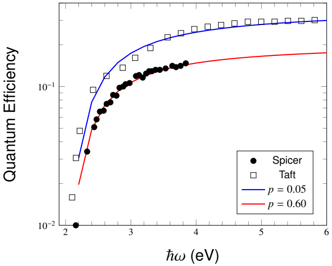

Cs_3Sb: $E_g = 1.6$ eV, $E_a = 0.4$ eV, $R = 0.2$

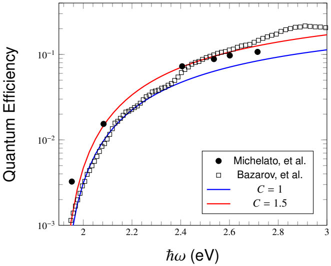

K_2CsSb: $E_g = 1.2$ eV, $E_a = 0.7$ eV, $R = 0.2$

Dielectric Parameters

- Laser penetration depth $\delta(\omega)$ and reflectivity $R(\omega)$

$$R(\omega) = \frac{(n-1)^2 + k^2}{(n+1)^2 + k^2}$$
$$\delta(\omega) = \frac{c}{2k\omega} \quad (10)$$

- Get n and k from exp. data OR[a] Bound (Lorentz) $\hat{\varepsilon}_b$ & free (Drude) $\hat{\varepsilon}_f$

$$\hat{\varepsilon}(\omega) = \varepsilon_0 \left(n^2 - k^2 + 2ink\right)$$
$$\equiv \hat{\varepsilon}_f + \hat{\varepsilon}_b$$

$$\hat{\varepsilon}_f(\omega) = 1 - \frac{f_0\ \omega_p^2}{\omega(\omega + i\ \Gamma_0)} \quad (11)$$

$$\hat{\varepsilon}_b(\omega) = \sum_{j=1}^{n} \frac{f_j\ \omega_p^2}{(\omega_j^2 - \omega^2 - i\omega\Gamma_j)}$$

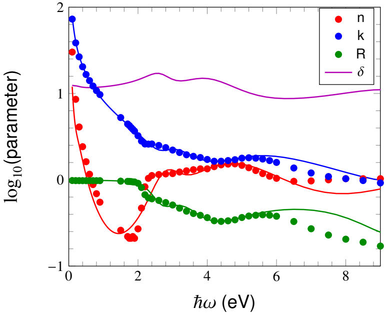

Term	Unit	$j=0$	$j=1$	$j=2$	$j=3$	$j=4$
f_j	-	0.575	0.061	0.104	0.104	0.638
$\hbar\Gamma_j$	eV	0.030	0.378	1.056	1.056	4.305
$\hbar\omega_j$	eV	10.83	0.2910	2.957	2.957	11.18

TABLE: Copper Lorentz-Drude parameters for Eq. (11)

[a] K.L. Jensen, D. Finkenstadt, A. Shabaev, S.G. Lambrakos, N.A. Moody, J.J. Petillo, H. Yamaguchi, and F. Liu, J. Appl. Phys. **123**, 045301 (2018).

Discrete Shell Model

- Energy: $E = \hbar\omega - E_g \rightarrow v_o = \sqrt{2E/m}$
  time: $t_{n-j} = (n-j)\Delta t$ (t_n is present)
  $x_l = -(j - 1/2)\Delta x$ for $l \in (1 \cdots N_x)$
  s = # of scatterings
  at every τ all e^- scatter: $E \rightarrow E - \Delta E$, $v \rightarrow v_s$
- Every time step (n): Spheres of charge $\Delta Q_l(n)$ from laser intensity $I_\lambda(t)$ and penetration $e^{-x/\delta}$ start expanding

$$J_{lj}^s(n) = J_o\; W_{n-j}\; S_l^s\; F_{lj}^s\; D_{lj}^s(n)$$

$$J_{total}(t_n) = \sum_{ljs} J_{lj}^s(n) \qquad (12)$$

- J_o contains all dimensioned coefficients;
  $W_j = I_\lambda(t_j)/I_o$ is ratio of laser intensity to max;
- S_l^s = weighting for l^{th} shell after s events;
- F_{lj}^s = emitted fractional charge due to l^{th} sphere t_j after creation and s scatterings
- $D_{lj}^s(n)$ = transmission probability at t_n for l^{th} shell created t_j before present t_n after s scatterings

Each factor has specific model[a]

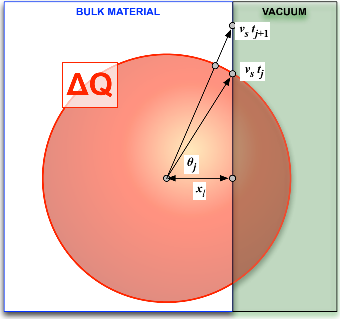

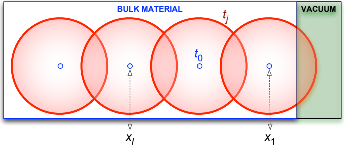

Photocurrent = $\sum$ (expanding spheres reaching surface and satisfying $D(E)$)

[a] K.L. Jensen, J.J. Petillo, D.N. Panagos, S. Ovtchinnikov, N.A. Moody J. Vac. Sci. Technol. B**35**, 02C102 (2017).

Long Time Tails and Emission

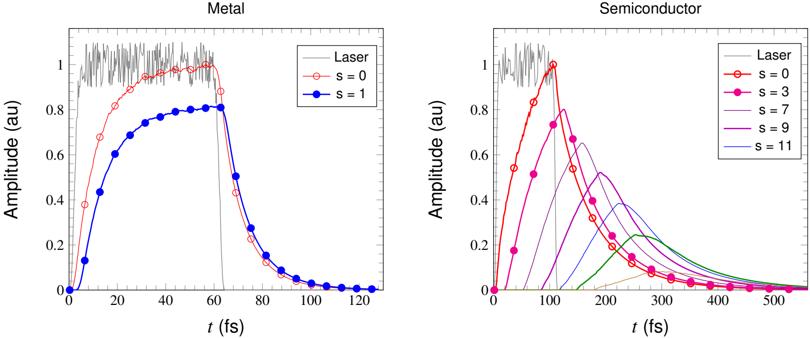

- (left) Metals: δ is short; two scatterings render e^- emission-ineligible
- Semiconductors: δ is deeper, many scatterings allowed, letting more S_l^s factors contribute such that $J(n)$ acquires "drift-diffusion-like" characteristic seen in **exps.**
  P. Hartmann, J. Bermuth, *et al.*, J. Appl. Phys. **86**, 2245 (1999); I.V. Bazarov, *et al.*, Phys. Rev. ST-AB **11**, 040702 (2008)

K.L. Jensen, J.J. Petillo, D.N. Panagos, S. Ovtchinnikov, and N.A. Moody, J. Vac. Sci. Technol. B **35**, 02C102 (2017).

Time-Dependent Surface Field and Scattering (Delay)

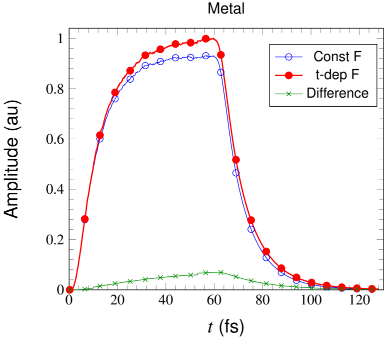

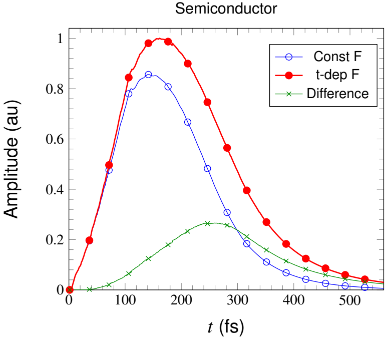

- Total current $J(n)$ as per Eq. (12) ($\sum J^s_{lj}(n)$) without (blue) and with (red) a time-dependent increasing surface electric field. Laser jitter = 10%.
- Delayed e^- take longer to get to surface, experience a smaller barrier (Schottky effect) so a t–dependent simulation reveals contribution to yield
- Metals: delayed contribution is small
  Semiconductor: many e^- scattered so delayed effect is prominent

Sections Outline

Density Functional Theory DOS (LDA)

- Density of States (general):

$$\mathcal{D}_0(E) = V\left(\frac{m_n}{\pi^2\hbar^3}\right)\sqrt{2m_n E}; \qquad \mathcal{D}_\alpha(E) = \mathcal{D}_0(E)\,(1+2\alpha E)\,\sqrt{1+\alpha E} \qquad (13)$$

- DFT can augment spectral data bases for density of states $\mathcal{D}(E)$ and optical parameters $\delta(\omega)$ and $R(\omega)$, and allows path forward when data is unavailable

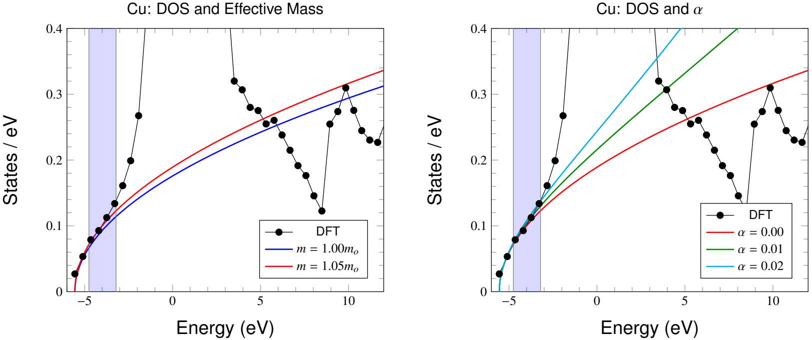

D. Finkenstadt, S.G. Lambrakos, K.L. Jensen, A. Shabaev, N.A. Moody, "Calc. of Density of States...", Proc. of SPIE, San Diego, CA, 2017).
D. Finkenstadt, S.G. Lambrakos, K.L. Jensen, A. Shabaev, N.A. Moody, "DOS of Cs3Sb ...", Proc. of SPIE, San Diego, CA, 2017).

Optical Constants and Fitting

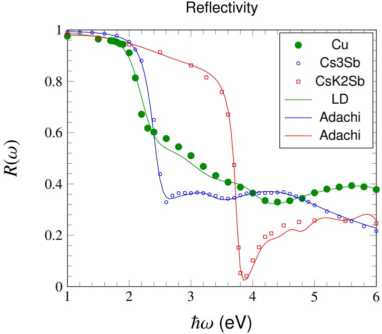

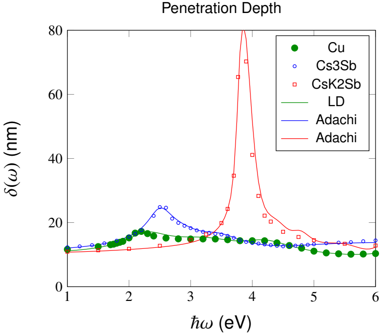

- Metals: Lorentz-Drude with Gaussian broadening function
- Semiconductors: Adachi Model
- Theory: based on code developed by Dr. Oksana Chubenko (GWU, ASU)

Airy Transfer Matrix Approach

TMA for triangular barrier: matrix equation relates the reflection (r) and transmission (t) coefficients for potential regions with field $V(x) = V_o - Fx$

$$\psi(x) = t(k)\, Zi(c,z) + r(k)\, Zi(-c,z), \qquad z = |k_o^2 - k^2 - fx|/f^{2/3} \tag{14}$$

Match Wave function and first derivative at boundary:

$$\begin{pmatrix} 1 & 1 \\ ik & -ik \end{pmatrix}\begin{pmatrix} 1 \\ r(k) \end{pmatrix} = \begin{pmatrix} \mathrm{Zi}(i,z_o) & \mathrm{Zi}(-i,z_o) \\ \mathrm{Zi}'(i,z_o) & \mathrm{Zi}'(-i,z_o) \end{pmatrix}\begin{pmatrix} t(k) \\ 0 \end{pmatrix} \tag{15}$$

Generalization to multiple transitions:[a]

$$M_{n-1}(x_n) \cdot \zeta_{n-1}(x_n) = M_n(x_n) \cdot \zeta_n(x_n)$$

$$\zeta_{n-1}(x_n) \equiv \hat{S}(n) \cdot \zeta_n(x_n)$$

$$\mathrm{Zi}(c,z) = \frac{H_c(z^{-3/2})}{2\sqrt{\pi}} z^{-1/4} \exp\left(\frac{2}{3} c z^{3/2}\right)$$

Transmission: $D(k) = (f^{1/3}/\pi k)\, |t(k)|^2$

$$t(k) = \left\{ \left[\prod_{n=1}^{N} \hat{S}(n) \right]_{1,1} \right\}^{-1}$$

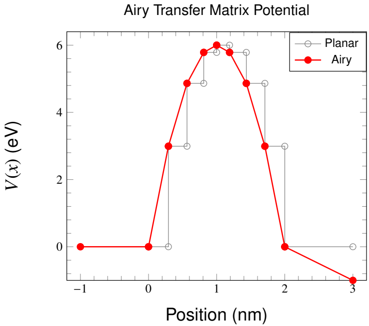

[a] K.L. Jensen, D. Finkenstadt, A. Shabaev, S.G. Lambrakos, N.A. Moody, J.J. Petillo, H. Yamaguchi, and F. Liu, J. Appl. Phys. **123**, 045301 (2018).

DFT and Pöschl-Teller (sech^2) Wells

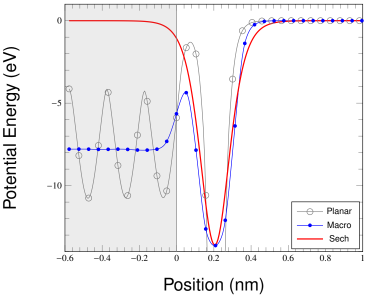

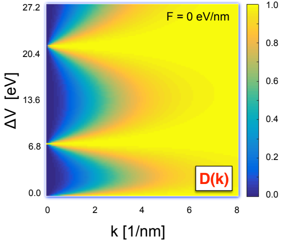

PT wells are reflectionless for $\Delta V = \hbar^2 \nu(\nu+1)/2ma^2$ (integer ν), but in between, they mimic a triangular barrier (height V_b chosen to minimize least squares difference)

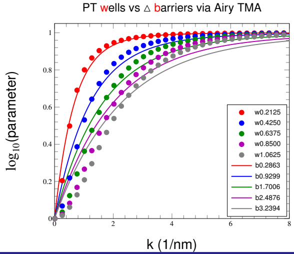

Planar $V(x)$ of graphene on Cu using DFT

Macro Macro-averaging of Planar DFT $V(x)$

Sech Hyperbolic-secant potential (for Airy-TMA):

$$V_{pt}(x) \equiv -\Delta V \,\mathrm{sech}^2\left[\frac{x - x_o}{a}\right] \qquad (16)$$

where $x_o = r_{Cu} + r_C = 0.15875$ nm,
$a = r_n = n\hbar/m\alpha_{fs}c \equiv n a_o$ for $n = 2$, and
$\Delta V = R_y = m(\alpha_{fs}c)^2/2 = 13.606$ eV

GRAPHENE V(X) AND AIRY TMA

K.L. Jensen, D. Finkenstadt, D.A. Shiffler, A. Shabaev, S.G. Lambrakos, N.A.A. Moody, and J.J. Petillo, J. Appl. Phys. **123**, (2018).

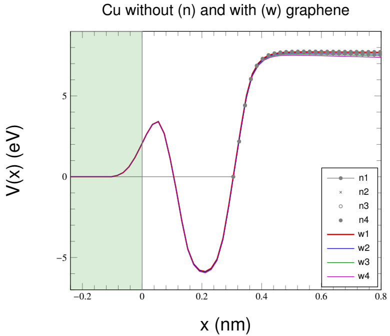

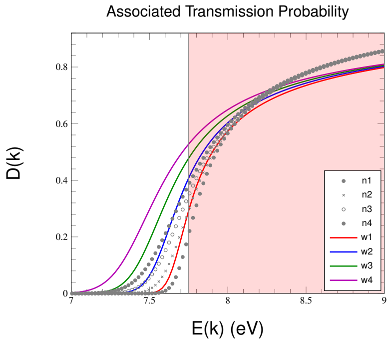

Left DFT Potential for Graphene on Cu (shaded green): $V(x)$ shown with (w_j) and without (n_j: $V(x < x_s) \equiv 0$, $x_s = 0.305$ nm) well region. Surface field: $F_j(x > x_s) = (0.125, 0.25, 0.375, 0.5)$ eV/μm for $j \in (1, 2, 3, 4)$ (photoinjector-like).

Right Associated $D(k)$ using same labeling. Shaded red is region of "over barrier" emission: observe impact of *ad hoc* surface field

Analogous behavior shown to occur with rectangular, triangular, and parabolic barriers

Resonant vs. Reflectionless

Study of □, △, ⋂ and well/barrier potentials reveal analogous behavior to Cu-Graphene [a]

Gray = wells (L_w, V_w) Yellow = barriers (L_b, V_b)

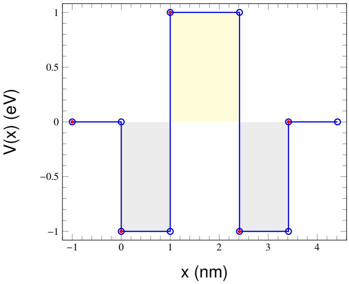

Demand $\hbar^2\kappa_{bw}^2/2m = V_b - V_w$ (V_b can be + or -).

Let $\kappa_s = \sqrt{2mV_s}/\hbar$. If $V_w = -V_b$, then $L_w = \sqrt{2}\, L_b$

$$2\kappa_w L_w \sim \kappa_{bw} L_b \rightarrow L_b = 2L_w \left[\frac{V_w}{V_b - V_w} \right]^{1/2} \quad (17)$$

[a] K. L. Jensen, D. Finkenstadt, D. A. Shiffler, A. Shabaev, S. G. Lambrakos, N. A. Moody, J. J. Petillo, JAP **123**, 045301 (2018)

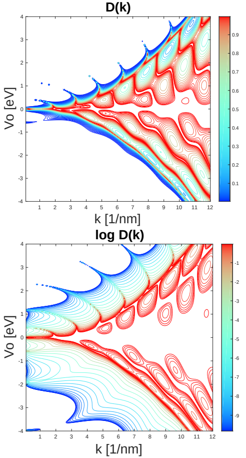

Two circumstances exist for which $D(k) \rightarrow 1$:

- discrete values of k for $V_b = 0$ and $V_w > 0$ (resonant or RTD-like), and
- discrete values of $V_b < 0$ for all k with $V_w = 0$ (reflectionless or PT-like)

Surface Roughness, Dark Current, Trajectories, Statistics

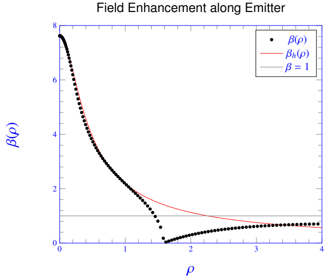

$\beta(\rho)$ = Point charge model; $\beta_h(\rho)$ = hyperbolic approx.

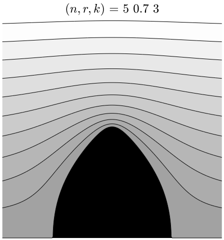

Center Emitter in Point Charge Model

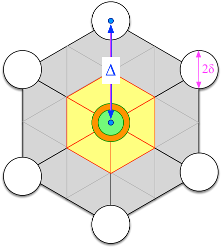

Field Thermal-Field Thermal

above Field enhancement as function of radial position for center emitter on right (including shielding); $\beta_h(x)$ = hyperbolic approx. Used in tip current model of Fig. 1

right Point Charge Model of meso-scale emitters with micro-scale emission sites which can exhibit field, T-F, and thermal emission areas simultaneously.
Similar analysis possible for field → photo;
enables unit cell trajectory analysis, random site

Concluding Remarks

Basic Photoemission Model

1. Neglect of Scattered electron contributionm (“Fatal Approximation”)
2. Energy parabolic in k; simple DOS, optical, scattering parameters $(\delta(\omega), \tau(E))$
3. Moments Model (analogous to 3-Step) uses step function $D(k)$ (Fowler-Dubridge approx)

Modifications to Basic Model in PIC

1. Delayed emission model and contribution of scattered electrons[a]
2. Improved $D(k)$ model and surface barrier for semiconductors
3. Improved optical parameters (Lorentz-Drude and Adachi)

[a] K.L. Jensen, J.J. Petillo, S. Ovtchinnikov, D. Panagos, *et al.*. “*Modeling emission lag after photoexcitation.*” J. Appl. Phys., **122(16)**, 164501, 2017.

New Physics Under Development

1. Density Functional Theory (DTS) used to determine effective mass m_n, density of states $\mathcal{D}(E)$, Fermi level μ, band gap E_g, optical constants (n, k), reflectivity (R), laser penetration depth (δ)[a]
2. Emission probability $D(k)$ for coatings provided by Airy Transfer Matrix Approach [b]
3. Surface Roughness, Emittance, trajectories, thermal-field dark current in Unit Cell

[a] D. Finkenstadt, S.G. Lambrakos, K.L. Jensen, *et al.*. Proc. SPIE, 2017; *ibid*, Proc. SPIE, 2017.
[b] K.L. Jensen, D. Finkenstadt, A. Shabaev, S.G. Lambrakos, N.A. Moody, J.J. Petillo, H. Yamaguchi, F. Liu. J. Appl. Phys., **123(4)**, 045301, 2018.

Bibliography I

- K.L. Jensen, *Electron Emission Physics: Advances in Imaging and Electron Physics* (Elsevier, San Diego, CA, 2007).
- K.L. Jensen, *Introduction to the Physics of Electron Emission* (John Wiley & Sons, Inc., Hoboken, New Jersey, 2017).
- K.L. Jensen, N.A. Moody, D.W. Feldman, E.J. Montgomery, and P.G. O'Shea, J. Appl. Phys. **102**, 074902 (2007).
- K.L. Jensen, B. Jensen, E.J. Montgomery, D.W. Feldman, P.G. O'Shea, and N.A. Moody, J. Appl. Phys. **104**, 044907 (2008).
- K.L. Jensen, E.W. Montgomery, D.W. Feldman, P.G. O'Shea, J.R. Harris, J.W. Lewellen, and N. Moody, J. Appl. Phys. **110**, 034504 (2011).
- K.L. Jensen, D.A. Shiffler, J.J. Petillo, Z. Pan, and J.W. Luginsland, Phys. Rev. ST Accel. Beams **17**, 043402 (2014).
- D. Finkenstadt, S.G. Lambrakos, K.L. Jensen, A. Shabaev, and N.A. Moody, Proc. of SPIE, San Diego, CA, 2017).
- K.L. Jensen, D.A. Shiffler, M. Peckerar, J.R. Harris, and J.J. Petillo, J. Appl. Phys. **122**, 064501 (2017).
- K.L. Jensen, J.J. Petillo, D.N.A. Panagos, S. Ovtchinnikov, and N.A. Moody, J. Vac. Sci. Technol. B **35**, 02C102 (2017).
- D. Finkenstadt, S.G. Lambrakos, K.L. Jensen, A. Shabaev, and N.A. Moody, Proc. of SPIE, San Diego, CA, 2017).
- K.L. Jensen, J.J. Petillo, S. Ovtchinnikov, D. Panagos, N., N.A. Moody, and S.G. Lambrakos, J. Appl. Phys. **122**, 164501 (2017).
- K.L. Jensen, D. Finkenstadt, A. Shabaev, S.G. Lambrakos, N.A. Moody, J.J. Petillo, H. Yamaguchi, and F. Liu, JAP**123**, 045301 (2018).
- K.L. Jensen, IEEE Trans. Plas. Sci. **46**, 1881 (2018).
- K.L. Jensen, D. Finkenstadt, D.A. Shiffler, A. Shabaev, S.G. Lambrakos, N.A.A. Moody, and J.J. Petillo, J. Appl. Phys. **123**, (2018).